forests

MDPI

Article

Responses of Vegetation Phenology to Urbanization in Plateau Mountains in Yunnan, China

Mengzhu Sun [1,2], Kun Yang [1,2,*], Jiasheng Wang [1,2,*], Wenjing Ran [2,3] and Xun Rao [2,3]

[1] Faculty of Geography, Yunnan Normal University, Kunming 650500, China
[2] The Engineering Research Center of GIS Technology in Western China of Ministry of Education of China, Yunnan Normal University, Kunming 650500, China; rx5428@user.ynnu.edu.cn (X.R.)
[3] School of Information Science and Technology, Yunnan Normal University, Kunming 650500, China
* Correspondence: yangkun@ynnu.edu.cn (K.Y.); jersonwang@ynnu.edu.cn (J.W.)

Abstract: The process of urbanization alters the distribution of land use and gives rise to certain climatic modifications that have a direct influence on vegetation phenology. Mountainous areas have a fragile biological environment, and vegetation phenology is relatively sensitive to urbanization. However, there is a paucity of research on the impact of urbanization in mountainous areas on vegetation phenology. The Urban Agglomeration of Central Yunnan (UACY) is located on the Yunnan–Guizhou Plateau in China. This study explored the vegetation phenological changes in different terrains from 2001 to 2020 in the UACY based on remote sensing data. Using the dynamic gradient method, we examined the response of vegetation phenology to urbanization from three aspects: urban–rural gradient, urbanization intensity (UI), and population density. The results showed that landform has a significant impact on SOS (start of growing season), with a topographic relief difference of 200 m acting as the dividing line. The findings derived from the dynamic gradient analysis indicate that UI has the most significant effect. SOS advances by 5.77 days (R^2 = 0.96), EOS (end of growing season) advances by 2.30 days (R^2 = 0.83), and LOS (length of growing season) lengthens by 2.59 days (R^2 = 0.87) for every 10% increase in UI. This study has the potential to serve as a valuable resource for future urban planning and administration in the UACY. Additionally, it could provide decision-making support for the development of mountainous urban agglomerations in ecological environments.

Keywords: Urban Agglomeration of Central Yunnan; land surface phenology; urban expansion; impervious surface; population density

Citation: Sun, M.; Yang, K.; Wang, J.; Ran, W.; Rao, X. Responses of Vegetation Phenology to Urbanization in Plateau Mountains in Yunnan, China. *Forests* **2023**, *14*, 2347. https://doi.org/10.3390/f14122347

Academic Editor: Romà Ogaya

Received: 13 October 2023
Revised: 21 November 2023
Accepted: 27 November 2023
Published: 29 November 2023

1. Introduction

Urbanization, which includes the creation and spread of cities and towns, population expansion, urban life, etc., is a crucial aspect of current global development [1]. Accompanied by an increasing acceleration of urbanization, geographical expansion, population growth, economic development, and resource consumption will all have an impact on the ecological environment [2] and may cause habitat loss [3], a reduction in biodiversity [4], ecosystem degradation, soil erosion and desertification, biological invasion, and other problems. Vegetation phenology is an important surface parameter in atmospheric and climatic models because it is the mirror of the seasonal climatic cycle of vegetation in response to light, temperature, and rainfall. Vegetation phenology is also a vital variable in the research fields of ecosystem carbon balance [5,6], agricultural production [7], frost events [8], and tourism [9]. The spatio-temporal change in vegetation phenology and its response to climate change have become one of the hot spots in ecological research at present [10–13]. Urbanization is also one of the factors influencing vegetation phenological changes [14]. Urbanization-related expansion disrupts the distribution of heat and water, changing local microclimates and, as a result, the phenological processes of vegetation [15,16].

Extensive research has been conducted investigating the influence of urbanization on vegetation phenology based on remote sensing [17]. Studies have demonstrated a significant correlation between human activities and the proliferation of vegetation [18]. The indirect impacts of urban expansion on vegetation are contingent upon the intensity of urban development and population density [19]. The vegetation phenology shifted earlier for SOS and later for EOS in highly urbanized regions than in less urbanized areas [20]. There were significant differences in vegetation phenology between urban and rural areas [21,22]. And the density of an urban population shows a significant negative correlation with spring phenology and a positive correlation with autumn phenology [23]. However, previous research has concentrated on the influence of urban heat island or land surface temperature on vegetation phenology [24], overlooking additional variables associated with urban expansion. The majority of these studies primarily concentrate on cities situated on the plains [25], or have a large scale [26,27], and there are few studies on the response of vegetation phenology to urbanization in urban agglomerations on mountainous plateaus. Rapid urbanization in mountainous areas has a more complicated effect on the ecology than it does in plains [28,29]. Mountainous areas are crucial ecological functional zones, providing various ecosystem services for the people who live in and around them [30]. Simultaneously, they play a vital role in the Earth's biodiversity through a series of mechanisms, influencing adjacent lowlands through biological exchange, regional climate variations, and nutrient runoff [31,32]. Studying the impact of urbanization on vegetation phenology in mountainous urban areas is essential for ecological balance and biodiversity. Moreover, it has been suggested that elevational gradients constitute the most powerful tools to study triggers for phenological onset dates in mountainous areas using a space-for-time approach because such gradients provide a large set of different meteorological conditions with an identical photoperiod [33], whereas studies on the effects of urbanization on vegetation phenology rarely take altitude into account.

The Urban Agglomeration of Central Yunnan (UACY) has diverse topography and rich vegetation resources. It is the most economically developed region in Yunnan Province, which is one of China's carbon sinks [34]. Since 2011, when Yunnan Province announced its provincial strategy of "Protecting Farmland in Flatland Areas and Constructing Mountainous Cities" [35], Yunnan has changed its approach to land use for urban and rural construction, implemented the "Constructing Mountainous Cities" program, and directed its cities to develop on mountains and hills [36]. To improve comprehension of the effects of urbanization on vegetation phenology in the UACY, based on MODIS-EVI data, impervious surface, and population density, we extracted vegetation phenology parameters, explored the spatial pattern of vegetation phenology in various terrain types, and dynamically analyzed the response of vegetation phenology to urbanization in the UACY in the aspect of urban–rural gradient, UI, and population density. The objective of our study is to explore the following: (1) the trend of vegetation phenology during 2001–2020 in the UACY; and (2) the relationship between vegetation phenology and urban expansion in the UACY during 2001–2020.

2. Data and Methodology

2.1. Study Area

The UACY is located in the central-eastern part of Yunnan Province (23°20′–27°02′ N, 100°45′–104°48′ E), and includes Kunming City, Qujing City, Yuxi City, Chuxiong Yi Autonomous Prefecture, and 7 counties and cities in the north of Honghe Hani and Yi Autonomous Prefecture (Mengzi City, Kaiyuan City, Gejiu City, Mile City, Luxi County, Jianshui County, and Shiping County), with a total of 49 counties and cities covering an area of 111,400 km^2 (Figure 1). It is on a plateau with a low latitude, and most areas are at a high elevation, with more mountains and fewer plains. It is characterized by complex terrain and a three-dimensional climate. The average annual temperature is 16 °C, with summer temperatures usually between 25 to 30 °C and winter temperatures between 10 °C and 15 °C; the average annual precipitation is about 950 mm. As one of China's 19 national-level

urban agglomerations, the UACY lies at the intersection of "One Belt, One Road" and the Yangtze River Economic Belt. It is also an important part of China's "two horizontals and three verticals" development strategy. The UACY is the bellwether of economic and social development in Yunnan, where the economy has grown quickly over the past 20 years, with a dense population and transportation. According to the statistical yearbook of Yunnan Province [37], by the end of 2020, there were 21.96 million permanent residents, accounting for 46.5% of the province's total population. Its GDP increased from RMB 157.82 billion in 2001 to RMB 170.25 billion in 2020, increasing by almost 10 times. Statistics on the citizens in many cities changed from "registered population" to "permanent residents" between 2004 and 2005. This caused the total population of the UACY to grow quickly.

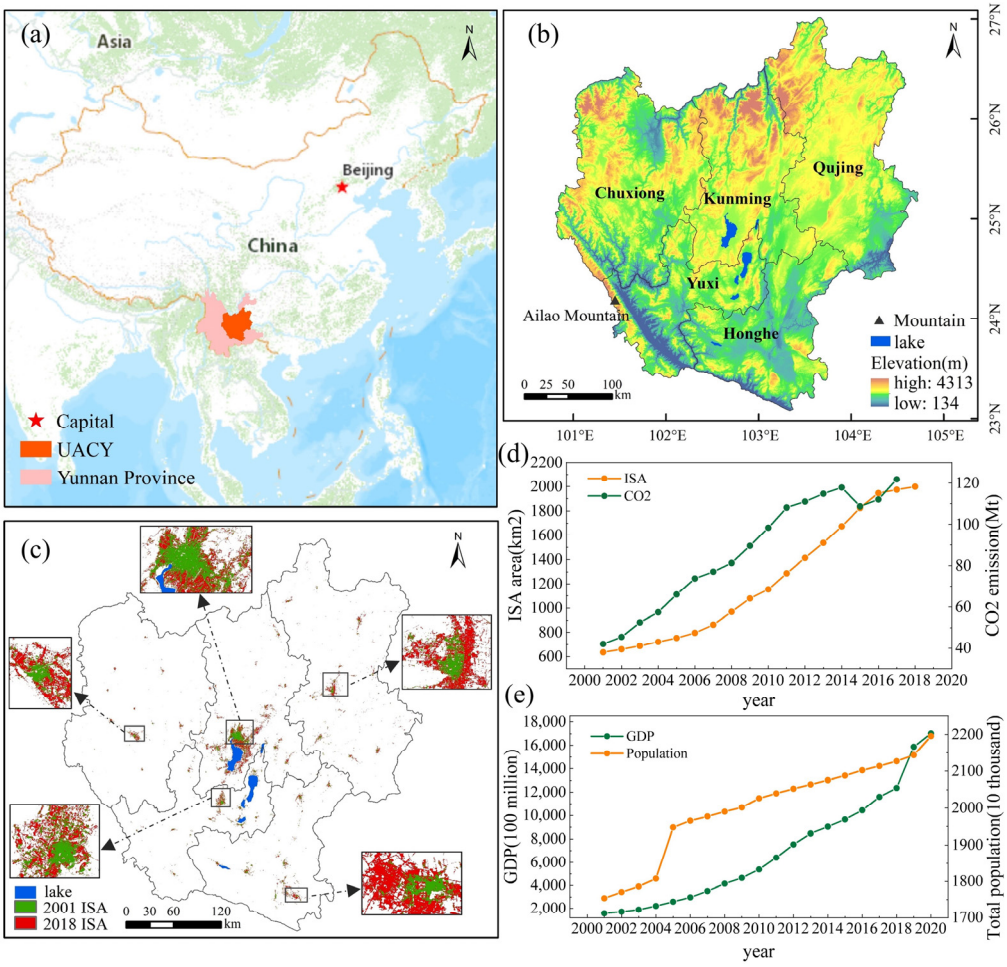

Figure 1. Study area, (**a**) location of UACY, (**b**) topography of UACY, (**c**) distribution of impervious surface in UACY in 2001 and 2018, (**d**) impervious surface area and CO_2 emission trend of UACY, (**e**) GDP and total population trend on UACY.

2.2. Data Collection

The data used in this paper include landform data, vegetation index data, impervious surface data, and population density data (Table 1). Landform types in China are composed of 7 basic landform morphologies and 4 altitude levels for each morphological surface, forming 25 basic landform types [38]. This study used the results of basic landform morphologies. The enhanced vegetation index (EVI) fixes problems with the normalized difference vegetation index (NDVI), especially soil background and saturation. It has better sensitivity in regions with a higher biomass than NDVI, and it eliminates the influence of the canopy [39]. It is therefore widely used in research on urbanization's effects on vegetation phenology [25,40]. The global artificial impervious area (GAIA) is the longest

temporal coverage currently available for artificial impervious areas in the world [41] and is widely used in studies related to urbanization [19,42].

Table 1. Data resources.

Type of Data	Resolution	Data Description	Data Sources
Landform data	1 km	China's topographic map at 1:1 million scale	https://www.resdc.cn/Default.aspx (accessed on 3 March 2023)
Vegetation index	250 m	MOD13Q1, from 2000 to 2021, 503 images, temporal resolution: 16 days,	https://www.earthdata.nasa.gov/ (accessed on 30 July 2022)
Impervious surface	30 m	GAIA, from 1985 to 2018	http://data.ess.tsinghua.edu.cn/ (accessed on 1 September 2022)
Population density	1 km	LandScan, from 2001 to 2020	https://www.satpalda.com/product/landscan/ (accessed on 1 September 2022)

2.3. Methodology

2.3.1. Extraction of Vegetation Phenology Parameters

(1) Reconstruction of MODIS EVI time-series data

The EVI curve displays erratic and uneven oscillations, limiting its direct use for trend analysis and information extraction. This limitation arises from factors such as sensor performance, meteorological impacts (e.g., clouds and aerosols), and variations in observation circumstances. It is necessary to apply denoising and smoothing techniques to the time-series vegetation index data in order to rebuild the time-series vegetation index [43]. In this study, the Savitzky–Golay (S–G) filter smoothing algorithm is used to reconstruct the time series vegetation index, and the formula is as follows:

$$Y_j^* = \frac{\sum_{i=-m}^{i=m} C_i Y_{j+1}}{N}. \quad (1)$$

In the formula, Y is the original EVI value, Y^* is the filter fitting value of EVI, j is the $j-th$ point of the data sequence, C_i is the filtering coefficient of the $i-th$ point data, and N is the width of the sliding window, that is $2 \times m + 1$.

(2) Extraction of phenological parameters

The phenological parameters were extracted using the dynamic threshold method, where 20% of the amplitude on either side of the vegetation index growth curve is taken as the start of growing season (SOS) and the end of growing season (EOS), and the duration between these two points defines the length of growing season (LOS). We only consider the case where a single growing period occurs throughout a year (for regions with two growing periods, we extract the one with the largest EVI among the vegetation growth periods in the area) in order to comprehensively analyze the vegetation phenology period and trend macroscopically [44]. The phenological formula is as follows:

$$\begin{aligned} EVI(SOS) &= (EVI_{\max} - EVI_{\min 1}) \times 20\% \\ EVI(EOS) &= (EVI_{\max} - EVI_{\min 2}) \times 20\% \\ EVI(LOS) &= EVI_{EOS} - EVI_{SOS} \end{aligned} \quad (2)$$

where $EVI_{\max}$ is the maximum of EVI in a year, and $EVI_{\min}$ is the minimum of EVI in the rising and falling phases, when EVI rises or falls by 20%, SOS and EOS are calculated, respectively.

2.3.2. Analysis of Spatio-Temporal Trend of Vegetation Phenology

The Theil–Sen Median method [45,46] was used to calculate the trend of vegetation phenology in the UACY during 2001–2020. The basic idea of this method is to estimate the value of the slope parameter in a univariate linear regression model by the utilization of the

median of the slopes obtained by solving for the slope using two sets of observations. This method is a reliable nonparametric statistical computation method which is often paired with the Mann–Kendall test [47], with excellent calculation efficiency and insensitivity to outliers. The formula of the Theil–Sen Median method is as follows:

$$\beta = mean(\frac{x_j - x_i}{j - i}), \forall j > i. \quad (3)$$

2.3.3. Analysis of the Impact of Urbanization on Vegetation Phenology

(1) Impact of land urbanization on vegetation phenology

The impact of impervious surfaces on vegetation phenology was analyzed dynamically using the urban–rural gradient and urbanization intensity (UI). The urban–rural gradient method builds buffer zones of 1 km, 2 km, 5 km, 10 km, 15 km, 20 km, and 25 km around the built-up area, with areas within 1–20 km as suburbs and 20–25 km as rural areas, taking into account the impact of physical distance. We used Global Urban Boundary (GUB) data as built-up area data, which were extracted using GAIA [48], due to the availability of GAIA with a time resolution from 2001 to 2018 and GUB data only being updated to 2018. In this study, we used the built-up areas for the years 2000, 2005, 2010, 2015 and 2018 as urban areas for the periods 2001–2004, 2005–2009, 2010–2013, 2014–2017, and 2018–2020, respectively.

The calculation of UI based on ISA is capable of capturing the gradual acclimation of vegetation to the dynamic urban environment. Using the method proposed by Jia et al. [20], UI is defined as the proportion of impervious surface area (ISA) in a pixel of 900 m × 900 m, and the value of UI is 0%–100%. In ArcGIS, we initially created a fishnet of 900 m × 900 m and then used the zonal statistics tool to calculate the number of 30 m impervious surface pixels within each 900 m × 900 m grid. The UI was calculated by dividing the count by the total number of pixels. We calculated the annual UI within the administrative boundary of the UACY from 2001 to 2020. Similarly, impervious surface data were only collected in 2018, and the UI for 2019 and 2020 was calculated using data from 2018. In the end, UI data were converted into vector data, and vegetation phenology corresponding to different UI levels was extracted. The impact of UI on vegetation phenology was calculated using the following equation:

$$\begin{aligned} \hat{SOS} &= \alpha_{SOS} + \beta_{SOS} UI \\ \hat{EOS} &= \alpha_{EOS} + \beta_{EOS} UI \\ \hat{LOS} &= \alpha_{LOS} + \beta_{LOS} UI \end{aligned} \quad (4)$$

where β_{SOS}, β_{EOS}, and β_{LOS} (days per 10% UI) are the response of vegetation phenology to impervious expansion and α_{SOS}, α_{EOS}, α_{LOS} are the influence of other factors on vegetation phenology besides UI.

(2) Impact of population on vegetation phenology

According to the population density classification method proposed by Ge et al. [49], the population density data of the UACY in the past 20 years were classified into 9 groups. This method reclassified the initial population density through the geographical proximity principle of a curve population gravity and obtained a population density that had the spatial clustering characteristic. The types of each group and the specific classification standards are presented in Table 2.

We extracted vegetation parameters (SOS, EOS, and LOS) at various population densities within the administrative boundary of the UACY year by year from 2001 to 2020 and analyzed the changes in each vegetation parameter at different population densities so as to analyze the impact of population on vegetation phenology.

Table 2. Standard of population density classification.

Rank	Type	Value	Rank	Type	Value
1	basic no-man's land	0–1	6	low concentration zone	201–400
2	extreme sparse area	2–25	7	moderate concentration zone	401–500
3	sparse area	26–50	8	high concentration zone	501–1000
4	relatively sparse area	51–100	9	the concentration core zone	>1000
5	general transition zone	101–200			

3. Results

3.1. Spatial Pattern of Vegetation Phenology in UACY

Figure 2 shows the distribution of phenology and its changes. In terms of temporal variation, the SOS has a trend of being delayed in the past 20 years in the UACY. As for its spatial distribution, the SOS in Kunming's urban area, south of Qujing and Honghe, is the earliest, whereas the EOS is the earliest near Ailao Mountain. In addition, the LOS was longer in southern Qujing and southern Honghe, where the altitude is lower, the water and heat are sufficient, and the vegetation growth time is longer.

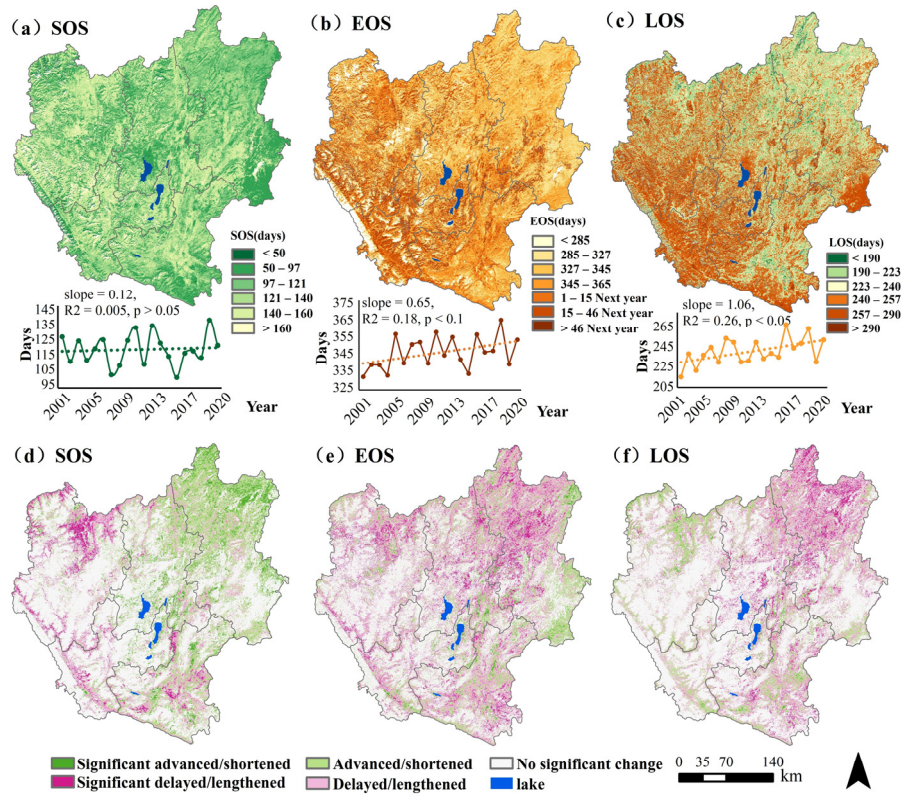

Figure 2. The distribution of vegetation phenology and significance level of changes in vegetation phenology in UACY from 2001 to 2020, (**a**–**c**) distribution of SOS, EOS, and LOS, respectively, (**d**–**f**) significance level of vegetation phenology change in SOS, EOS, and LOS, respectively.

The mean values of vegetation phenology in different landforms in the UACY from 2001 to 2020 are shown in Table 3. As a whole, with the increase in elevation and relief, the SOS and EOS are advanced, and the LOS is lengthened.

Table 3. Mean values of vegetation phenology in different landforms.

Terrain Types	SOS/Days	EOS/Days	LOS/Days
plain	123.32	352.23	242.18
plateau	126.93	353.13	231.55
hills	122.49	349.89	231.68
small undulating mountains	116.93	348.34	238.75
medium undulating mountains	116.64	348.78	244.53
large undulating mountains	110.76	339.30	245.90

As we can see from Figure 3, during 2001–2020, the SOS advanced 0.87 days/year ($p < 0.05$) whereas the EOS was delayed 0.22 days/year ($p > 0.05$) in the plain area. The SOS advanced 0.56 days/year ($p < 0.1$) in the plateau area, whereas the EOS was delayed 0.47 days/year on average ($p > 0.05$). In the hilly area, the SOS was delayed 0.14 days/year ($p > 0.05$), and the EOS was delayed 0.82 days/year ($p < 0.05$). The SOS and EOS were both delayed in the small undulating mountains, medium undulating mountains, and large undulating mountains, with the SOS being delayed 0.10 days/year ($p > 0.05$) and the EOS being delayed 0.65 days/year ($p < 0.1$) in the small undulating mountains; the SOS being delayed 0.44 days/year ($p > 0.05$) and the EOS being delayed 0.71 days/year ($p < 0.05$) in the medium undulating mountains; and the SOS being delayed 0.58 days/year ($p > 0.05$) and the EOS being delayed 0.58 days/year ($p > 0.05$) in the large undulating mountains. In general, the SOS of the UACY exhibits a pattern of being delayed over 20 years when the topographic relief is more than 200 m, whereas the SOS advances when the topographic relief is less than 200 m. All terrain types' EOSs showed a trend of being delayed during the past 20 years.

3.2. Responses of Vegetation Phenology to Urban Expansion

3.2.1. Trend of Vegetation Phenology on the Urban–Rural Gradient

Figure 4 illustrates the change in vegetation phenology along the urban–rural gradient in the UACY. From 2001 to 2020, the SOS in urban areas was significantly earlier than that in suburban and rural areas, and in general, the further away from the urban center, the later the SOS was. The SOS is 90.06 ± 10.82 days in urban areas, 118 ± 9.95 days in suburban areas, and 118.64 ± 9.02 days in rural areas (Figure 4a). In the UACY, the urban region has the earliest EOS, whereas the EOS in the suburban area is intermediate between the urban area and rural areas. The EOS in the urban area is 332.02 ± 8.82 d, 345.51 ± 10.70 days in the suburban area, and 346.40 ± 10.07 days in the rural area (Figure 4b). As can be seen from Figure 4c, the urban region of the UACY had a longer LOS than the suburban and rural areas, whereas the rural area's LOS was between the urban and suburban areas. The LOS is 248.96 ± 13.94 days in urban areas, 238.45 ± 14.34 days in suburban areas, and 239.40 ± 12.73 days in rural areas. The differences in land cover between urban, suburban, and rural areas are significant. Urban areas are primarily characterized by impervious surfaces, whereas rural areas consist of natural land surfaces and crops. Moreover, various regions exhibit distinct vegetation types, and different plant species have varying phenological patterns. These factors collectively contribute to the urban–rural disparities in the EOS and LOS.

3.2.2. Responses of Vegetation Phenology to UI

According to the urban–rural gradient method, the analysis of the impact of impervious surfaces on vegetation phenology only considers physical distance. However, in order to comprehensively reflect the acclimation of vegetation to the changing urban environment, vegetation phenology changes in the UACY were analyzed from the perspective of UI.

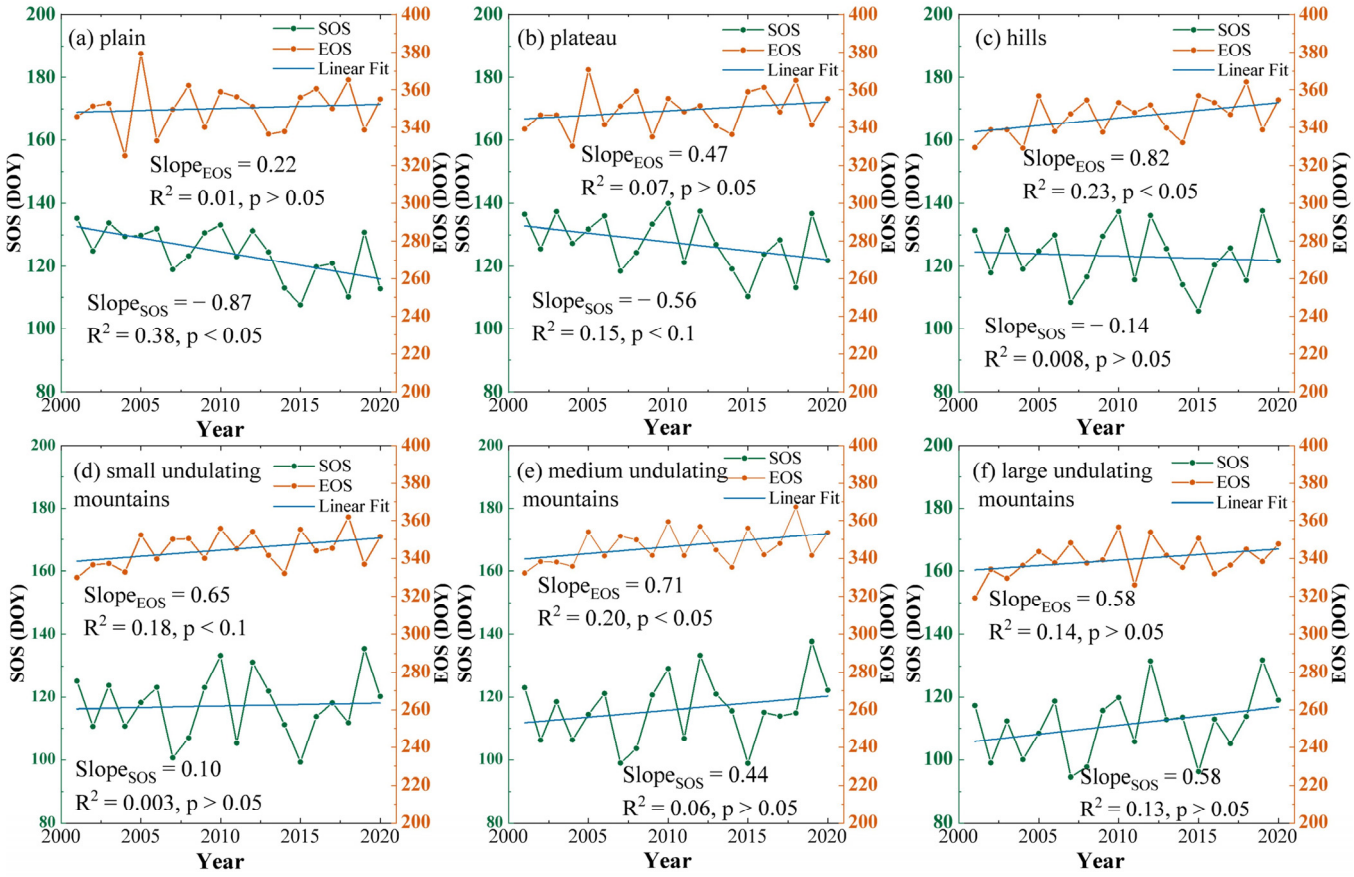

Figure 3. Changes in SOS and EOS for different landforms from 2001 to 2020.

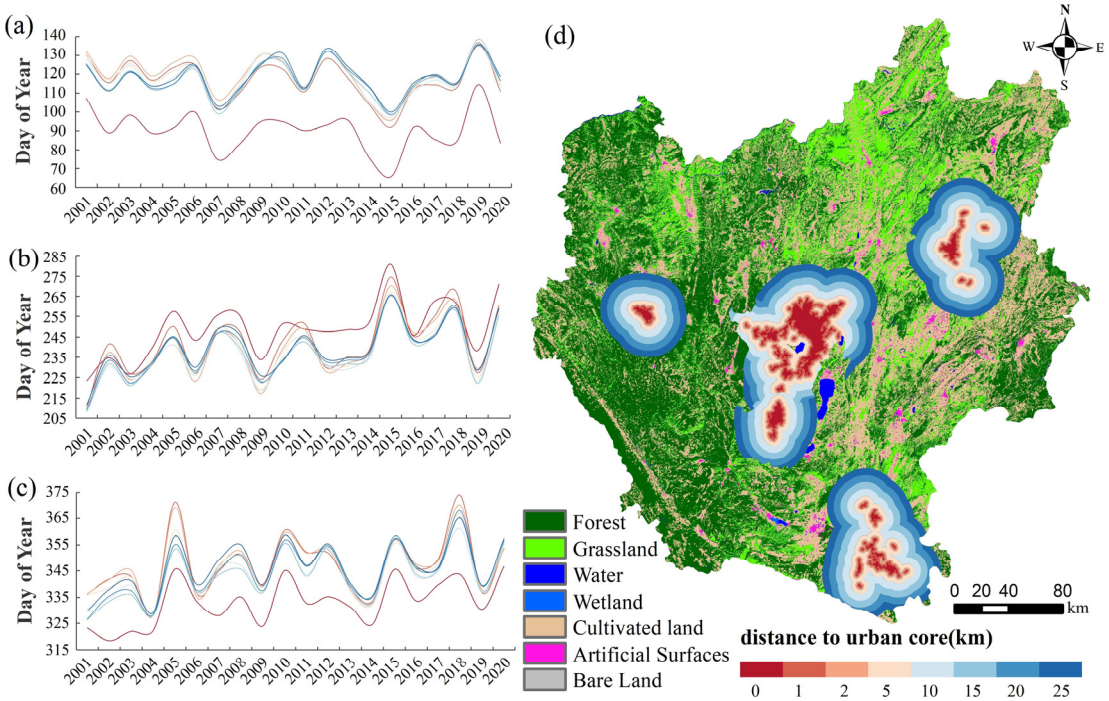

Figure 4. Changes in vegetation phenology in the urban and rural gradients of UACY, (**a**) changes in SOS in the urban–rural gradient, (**b**) changes in EOS in the urban–rural gradient, (**c**) changes in LOS in the urban–rural gradient, (**d**) land cover and different distance of buffers in urban–rural gradient of UACY in 2018.

For various cities, the district in the UACY where municipal administration is located was chosen as the study object. The response of vegetation phenology to ISA is shown in Figure 5. It is clear that various cities have varied vegetation phenology responses to ISA. Except for Honghe, the expansion of impervious surfaces in other cities has generally caused the SOS to advance, although Honghe had both an advanced and a delayed trend, which may be related to its topography (Figure 5a). Overall, the EOSs in five cities had a delayed trend, but the EOS in Chuxiong was advanced (Figure 5b), whereas the trend of the LOS also showed a bidirectional tendency (Figure 5c), which calls for further analysis.

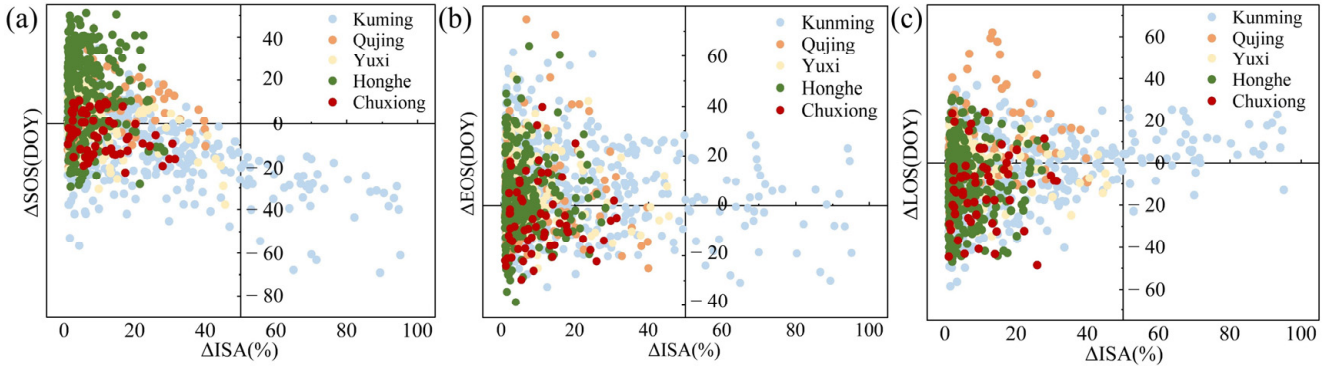

Figure 5. Scatter plot of ISA change and vegetation phenology change.

We reduced the data grid's scale for statistics to 900 m in order to conduct a more thorough trend analysis. We calculated the UI for each year and divided it into 10 categories according to the proportion at equal intervals. Subsequently, we counted vegetation phenology parameters in each category, and the results are shown in Figure 6. It can be seen that there are differences in the response of different vegetation phenology parameters to ISA, and all three phenology parameters responded significantly to UI. With an increase in UI, the SOS and EOS are significantly advanced and the LOS is significantly lengthened. Specifically, for every 10% increase in UI, the SOS advanced by 5.77 d (R^2 = 0.96, $p < 0.05$), the EOS advanced by 2.30 d (R^2 = 0.83, $p < 0.05$), and the LOS extended by 2.59 d (R^2 = 0.87, $p < 0.05$).

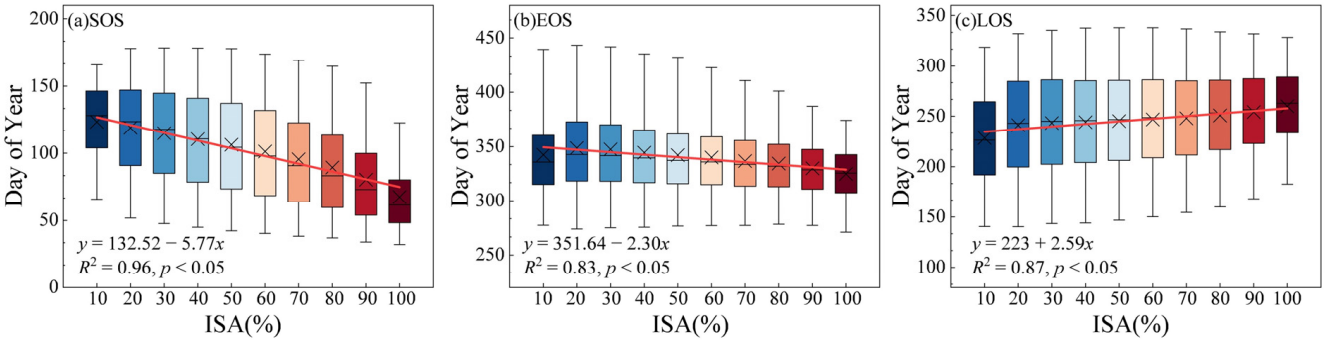

Figure 6. Responses of vegetation phenology to ISA in UACY from 2001 to 2020, "×" is the mean value, different colors represent different ISAs that match the values on the axis, (**a**) the responses of SOS to ISA, (**b**) the responses of EOS to ISA, (**c**) the responses of LOS to ISA.

3.2.3. Responses of Vegetation Phenology to Population

Figure 7 depicts the responses of vegetation phenology to population. The SOS in the basic no-man's land is the earliest (110.83 days), and then it becomes delayed with population growth. The SOS in the moderate concentration zone is the latest (125.40 days), and it advances from the moderate concentration zone to the concentration core zone. The EOS is the earliest (333.69 days) in the extreme sparse area, becomes delayed with population growth, and is the latest (348.12 days) in the moderate concentration zone. Like

the SOS, the EOS also shows a trend of advancement from the moderate concentration zone to the concentration core zone. However, LOS responds differently to population growth than the SOS and EOS. The LOS in the basic no-man's land is the longest (245.72 days), and as the population increases, the LOS shortens, with the relatively sparse area having the shortest LOS (217.53 days). Starting from the relatively sparse area, the LOS shows a general trend of lengthening with increasing population.

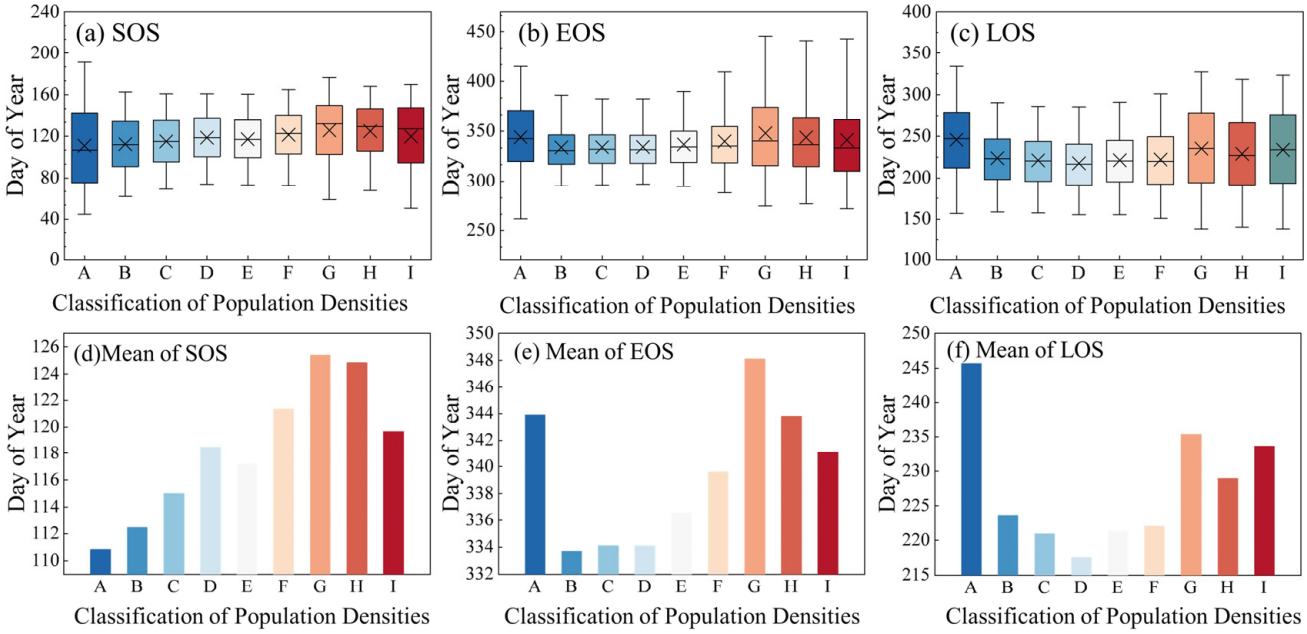

Figure 7. Responses of vegetation phenology to population density in UACY from 2001 to 2020, "×" is the mean value, A–I is the basic no-man's land, extreme sparse area, sparse area, relatively sparse area, general transition zone, low concentration zone, moderate concentration zone, high concentration zone, and concentration core zone, (**a**–**c**) is the box plot of vegetation phenology parameters of different population density types, (**d**–**f**) is the mean value of vegetation phenology in different population density types.

In summary, urban–rural differences, impervious surface expansion, and population density all have an impact on vegetation phenology in the UACY. Figure 8 shows the incidence of these three factors on vegetation phenology in the UACY.

The differences in regional phenology at different distances from urban areas are shown in Figure 8a,b. The SOS difference in the urban–rural gradient of UACY remains stable, as shown by the modest shift in ΔSOS. The difference in the EOS is similarly not particularly large, with the exception of 2001 and 2005. The impact of UI on vegetation phenology is shown in Figure 8c,d. In the past 20 years, with the increase in UI, vegetation phenology has changed significantly, especially the SOS. When $\Delta ISA \geq 40\%$, the SOS advances with increasing urbanization, and the impact of UI on the EOS is not as significant as on the SOS. When $\Delta ISA \geq 60\%$, the EOS advances with the strengthening of urbanization, but the advancement is not as large as that of the SOS. For the same ΔISA, when $\Delta ISA \geq 40\%$, the impact of UI on the SOS is stronger than the on the EOS (ΔSOS > ΔEOS). The impact of population on vegetation phenology is shown in Figure 8e,f. From 2001 to 2015, with the increase in population, the SOS was delayed, but the delayed trend gradually weakened with increasing years. In 2020, when $\Delta POP < 400$ person/km^2, the impact of population on the SOS does not show an obvious advanced trend, which was specifically manifested in that when ΔPOP increases, the changes in ΔSOS gradually decrease. When $\Delta POP \geq 400$ person/km^2, the SOS lengthened with the increase in population, and when the population density increased to a certain level, its impact on SOS gradually disappeared. The impact of population on the EOS is different from that on the SOS. In 2001, changes in

population density caused the EOS to be delayed, but from 2005 to 2020, with the increase in ΔPOP, the EOS advanced.

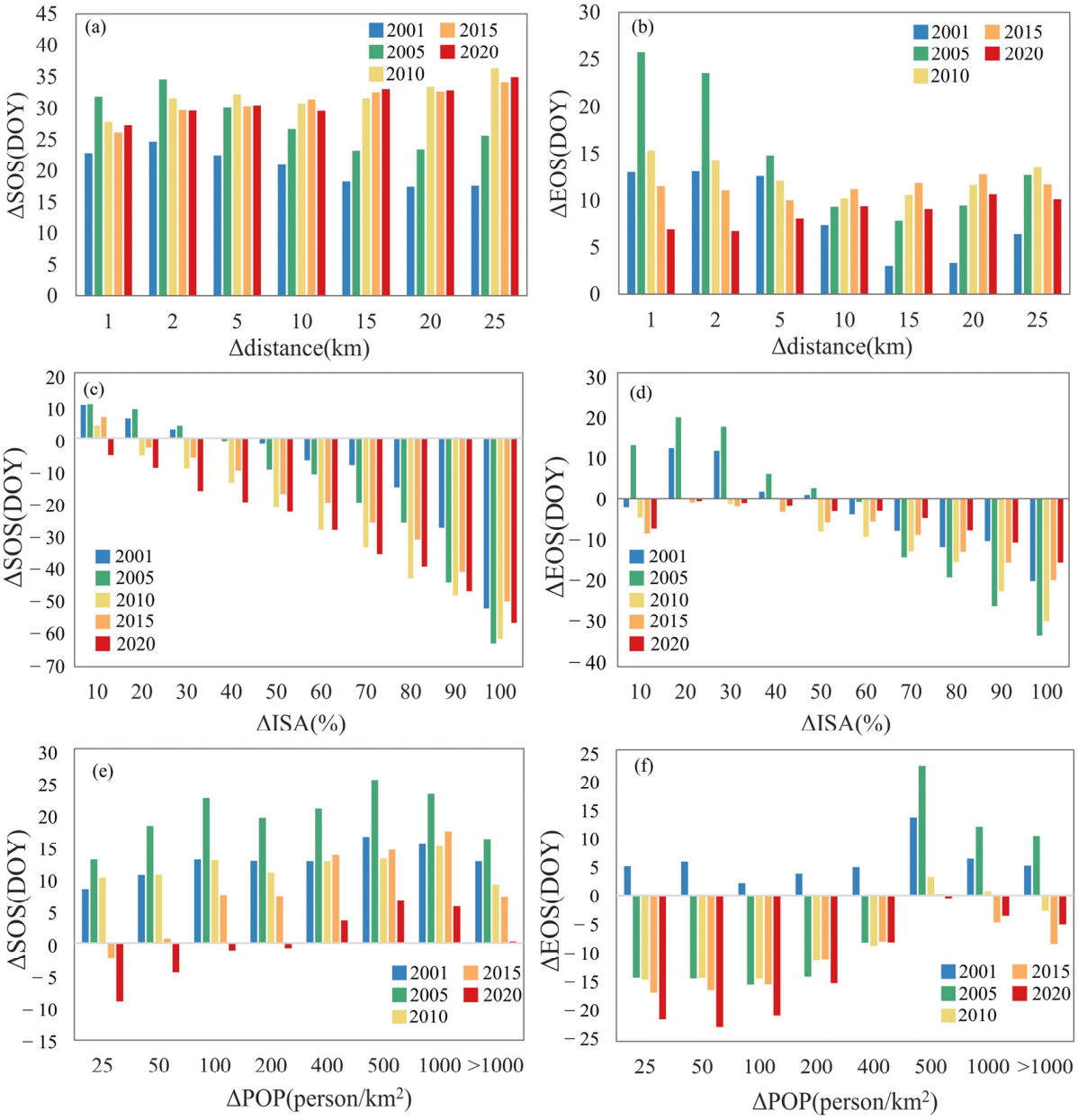

Figure 8. Impact of urbanization on vegetation phenology in UACY from 2001 to 2020, (**a**,**b**) the phenological difference of the urban–rural gradient, (**c**,**d**) impact of UI on vegetation phenology, (**e**,**f**) impact of population on vegetation phenology.

Overall, the impact of UI on vegetation phenology is more significant than that of the urban–rural gradient and population, and the impact on SOS is more significant than EOS.

3.3. Analysis of the Impact of the Altitude Gradient on Vegetation Phenology in UACY

The landscape of the UACY is tectonically complicated, in contrast to the plain cities, and most regions are at a higher altitude. In order to analyze the impact of altitude on urban vegetation phenology, the district where municipal governments are located in the UACY was taken as the study object, whose altitude ranges from 134 to 2877 m. An altitude gradient was built from 1000 to 2500 m at 100 m intervals in consideration of urban

expansion, so as to analyze the response of vegetation phenology to UI on the altitude gradient. The results are shown in Figure 9.

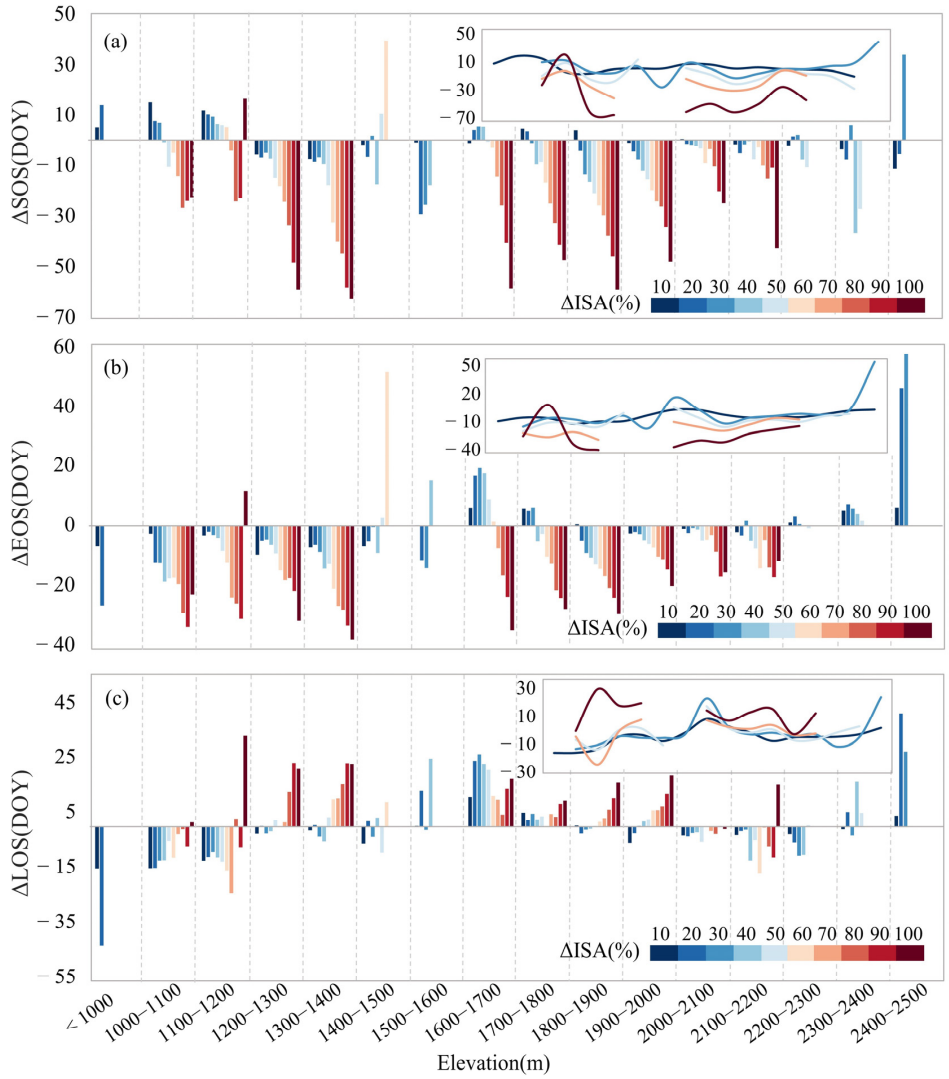

Figure 9. Response of vegetation phenology to UI on the altitude gradient in UACY from 2001 to 2020, (**a**) responses of SOS to UI on the altitude gradient, (**b**) responses of EOS to UI on the altitude gradient, (**c**) responses of LOS to UI on the altitude gradient.

When ΔISA = 10%, and the altitude is <1200 m, ISA expansion causes the SOS to be delayed. At altitudes within 1200–1700 m, ISA expansion causes the SOS to be advanced, and at altitudes >1900 m, ISA expansion also causes the SOS to be advanced. The tendency of the advancement became more and more pronounced with the increase in altitude. In contrast, the EOS was delayed at altitudes <1500 m, and the change showed a fluctuating trend at altitudes >1500 m. At altitudes <2400 m, the expansion of ISA resulted in a shortening of the LOS, and at altitudes >2400 m, the expansion of ISA resulted in a prolonged LOS. When ΔISA = 50%, ISA expansion mainly results in the advancement of SOS, and the effect is most significant at altitudes of 2300–2400 m. At the same time, the expansion of ISA mainly results in the advancement of the EOS, but the EOS was delayed at altitudes of 1400–1700 m. The expansion of ISA causes the shortening of the LOS, but the LOS is lengthened at altitudes of 1600–2000 m. When ΔISA = 100%, the expansion of ISA caused the SOS and EOS to advance, but the SOS and EOS were delayed in areas with an altitude of 1100–1200 m. At altitudes >1300 m, the impact of ISA on the SOS and EOS gradually weakened with the increase in altitude. The expansion of ISA mainly results in

the lengthening of the LOS, which was the most significant in the region of 1100–1200 m altitude, and the impact was gradually weakened with an increase in altitude.

4. Discussion

(1) Impact of landform on vegetation phenology

The results of this study suggest that SOS is greatly influenced by landform, with a topographic relief of 200 m as the dividing line, landform has a segmental impact on the SOS. The influences of light, temperature and water conditions, which are primary factors controlling vegetation phenology, have a substantial influence on vegetation phenology [50]. As altitude increases, there is a corresponding drop in temperature and air pressure. Additionally, ultraviolet radiation becomes comparatively stronger, while light intensity becomes somewhat diminished. The growth cycle of plants may be prolonged by the low temperature, delaying the SOS. A lower air pressure could affect the boiling point of water and the process of gas exchange in plant tissues, which would affect the growth of plants [51].

(2) Impact of impervious expansion on vegetation phenology

Impervious surfaces profoundly affect the regional hydrological cycle and energy balance as urbanization grows [52]. Impervious surfaces not only inhibit continuous gas exchange in the atmosphere–plant–soil system, but they also have an influence on important physiological activities in plants such as photosynthesis, respiration, and transpiration [53]. This study explored the impact of urbanization on vegetation phenology from the perspective of urban and rural gradient, UI, and population density. The results showed that UI had the greatest impact on vegetation phenology and a stronger impact on SOS. From 2009 to 2018, the increase in impervious surface area in the UACY exceeded 80 km^2/a [42]. Impervious surfaces have a high heat storage capacity and weak evaporation capacity, which impede the transport of air flow, resulting in the warming of a city [54]. Specifically, for every 1% increase in ISA, the temperature of the city rises by approximately 0.0219 °C [55]. Our study showed that for every 10% increase in UI, the SOS advances by 5.77 days, and the LOS lengthens by 2.59 days, this may be attributed to the increase in temperature.

In terms of spatial pattern, urban areas in Kunming, as the most urbanized area in the UACY, have the earliest SOS. This is due to the fact that vegetation phenology is closely related to light. It has been shown that changes in the natural cycle of light can have an impact on vegetation phenology [56]. According to Zheng et al., the substantial growth and extension of artificial light at night during urbanization disturbs the natural light cycle and leads to an early SOS [57]. Urbanization not only expands impervious surfaces in the 2D direction, but also in the 3D direction (i.e., increases in the height of buildings), which creates substantial ground shadow [58]. The alteration in light conditions in the vicinity of vegetation results in a consequential influence on the growth of vegetation.

Furthermore, our study showed that vegetation subjected to drought stress and water stress enters dormancy earlier, resulting in an advancement of the EOS by around 2.30 days. The phenomenon described may be attributed to the expansion of impervious surfaces, leading to turbulent processes that are more intense, moving surface water vapor higher, and increasing surface evaporation, which in turn causes a decrease in surface water vapor. Long term, this process takes the form of the "Urban Dry Island" (UDI) [59]. Impervious surfaces reduce soil permeability, making it difficult for precipitation to penetrate the soil quickly, resulting in water loss and increasing water stress for plants [60].

Changes in vegetation phenology are the result of multiple factors [61,62], and our findings offer essential details to evaluate the influence of urbanization on vegetation phenology [19,63]. Ecological factors, such as light, temperature, water and nutrients, have changed to varying extents in special metropolitan environments. In the future, ecological process models could be used to explain the mechanism of the impact of urbanization on vegetation phenology.

5. Conclusions

Understanding changes in vegetation phenology and its response to urbanization in urban agglomerations in mountain plateaus is of great significance for promoting regional environmental protection and economic development. In this study, we explored the spatial and temporal patterns of vegetation phenology and its response to urbanization in the UACY based on MODIS-EVI, impervious surface, population density, and topography data. We obtained the following findings: (1) The SOS is greatly affected by landform, with a topographic relief of 200 m as the dividing line, and landform has a segmental impact on the SOS. (2) UI has a more significant impact on vegetation phenology as with each 10% increase in UI, the SOS advanced 5.77 d, the EOS advanced 2.30 days, and the LOS lengthened 2.59 days. (3) In the process of urbanization, the expansion of impervious surfaces is the main factor affecting change in vegetation phenology. This study offers a quantitative basis for the impact of impervious surface expansion on vegetation phenology in plateau and mountainous urban agglomerations. However, the change in vegetation phenology is the result of multiple factors. In the future, ecological process models could be used to explain the mechanism of the impact of urbanization on vegetation phenology.

Author Contributions: Conceptualization, M.S., K.Y. and J.W.; Methodology, M.S.; Formal analysis, W.R.; Data curation, W.R. and X.R.; Writing—original draft, M.S.; Writing—review & editing, J.W.; Visualization, M.S. and X.R.; Supervision, K.Y. and J.W.; Project administration, K.Y. All authors have read and agreed to the published version of the manuscript.

Funding: This research was funded by the National Natural Science Foundation of China, grant number 42071381.

Data Availability Statement: The data presented in this study are available on request from the corresponding author.

Conflicts of Interest: The authors declare no conflict of interest.

References

1. Guangtao, W.; Fen, L.; Nannan, G.; Xiang, L. Perspective on study of urban science. *Bull. Chin. Acad. Sci.* **2022**, *37*, 177–187.
2. Han, G.; Xu, J.; Yuan, X. Impact of urbanization on vegetation phenology in major cities in Yangtze River Delta region. *Chin. J. Appl. Ecol.* **2008**, *19*, 1803–1809.
3. Ren, Q.; He, C.; Huang, Q.; Shi, P.; Zhang, D.; Güneralp, B. Impacts of urban expansion on natural habitats in global drylands. *Nat. Sustain.* **2022**, *5*, 869–878. [CrossRef]
4. Li, G.; Fang, C.; Li, Y.; Wang, Z.; Sun, S.; He, S.; Qi, W.; Bao, C.; Ma, H.; Fan, Y.; et al. Global impacts of future urban expansion on terrestrial vertebrate diversity. *Nat. Commun.* **2022**, *13*, 1628. [CrossRef] [PubMed]
5. Piao, S.; Ciais, P.; Friedlingstein, P.; Peylin, P.; Reichstein, M.; Luyssaert, S.; Margolis, H.; Fang, J.; Barr, A.; Chen, A.; et al. Net carbon dioxide losses of northern ecosystems in response to autumn warming. *Nature* **2008**, *451*, 49–52. [CrossRef]
6. Ge, Q.; Dai, J.; Zheng, J. The progress of phenology studies and challenge to modern phenology research in China. *Bull. Chin. Acad. Sci.* **2010**, *25*, 310–316. [CrossRef]
7. Qin, Y.; Liu, Y.; Ge, Q. Spatiotemporal variations in maize phenology of China under climate change from 1981 to 2010. *Acta Geogr. Sin.* **2018**, *75*, 906–916. [CrossRef]
8. Dai, J.; Wang, H.; Ge, Q. Changes of spring frost risks during the flowering period of woody plants in temperate monsoon area of China over the past 50 years. *Acta Geogr. Sin.* **2013**, *68*, 593–601.
9. Liu, J.; Li, Y.; Liu, H.; Ge, Q.; Dai, J. Climate chnage and peach blossom viewing: Impact and adaptation. *Geogr. Res.* **2016**, *35*, 504–512. [CrossRef]
10. Piao, S.; Liu, Q.; Chen, A.; Janssens, I.A.; Fu, Y.; Dai, J.; Liu, L.; Lian, X.; Shen, M.; Zhu, X. Plant phenology and global climate change: Current progresses and challenges. *Glob. Change Biol.* **2019**, *25*, 1922–1940. [CrossRef]
11. Shen, M.; Wang, S.; Jiang, N.; Sun, J.; Cao, R.; Ling, X.; Fang, B.; Zhang, L.; Zhang, L.; Xu, X.; et al. Plant phenology changes and drivers on the Qinghai–Tibetan Plateau. *Nat. Rev. Earth Environ.* **2022**, *3*, 633–651. [CrossRef]
12. Yu, L.; Liu, T.; Bu, K.; Yan, F.; Yang, J.; Chang, L.; Zhang, S. Monitoring the long term vegetation phenology change in Northeast China from 1982 to 2015. *Sci. Rep.* **2017**, *7*, 14770. [CrossRef] [PubMed]
13. Qiu, T.; Song, C.; Zhang, Y.; Liu, H.; Vose, J.M. Urbanization and climate change jointly shift land surface phenology in the northern mid-latitude large cities. *Remote Sens. Environ.* **2020**, *236*, 111477. [CrossRef]
14. Hu, Z.; Dai, H.; Hou, F.; Li, E. Spatio-temporal change of urban-rural vegetation phenology and its response to land surface temperature in Northeast China. *Acta Ecol. Sin.* **2020**, *40*, 4137–4145. [CrossRef]

15. Meng, D.; Liu, X.; Zhang, C. Responses of plant phenology to urban heat island effects in Beijing. *Chin. J. Ecol.* **2021**, *40*, 844–854. [CrossRef]
16. Liu, J.; Guo, H.; Zhang, L.; Lu, L. Impact of urbanization on vegetation phenology research in Beijing-Tianjin-Tangshan region. *Remote Sens. Technol. Appl.* **2014**, *29*, 286–292. [CrossRef]
17. Meng, L.; Mao, J.; Zhou, Y.; Richardson, A.D.; Lee, X.; Thornton, P.E.; Ricciuto, D.M.; Li, X.; Dai, Y.; Shi, X.; et al. Urban warming advances spring phenology but reduces the response of phenology to temperature in the conterminous United States. *Proc. Natl. Acad. Sci. USA* **2020**, *117*, 4228–4233. [CrossRef]
18. Su, F.; Fu, D.; Yan, F.; Xiao, H.; Pan, T.; Xiao, Y.; Kang, L.; Zhou, C.; Meadows, M.; Lyne, V.; et al. Rapid greening response of China's 2020 spring vegetation to COVID-19 restrictions Implications for climate change. *Sci. Adv.* **2021**, *35*, eabe8044. [CrossRef]
19. Zhang, L.; Yang, L.; Zohner, C.M.; Crowther, T.W.; Li, M.; Shen, F.; Guo, M.; Qin, J.; Yao, L.; Zhou, C. Direct and indirect impacts of urbanization on vegetation growth across the world's cities. *Sci. Adv.* **2022**, *8*, eabo0095. [CrossRef]
20. Jia, W.; Zhao, S.; Zhang, X.; Liu, S.; Henebry, G.M.; Liu, L. Urbanization imprint on land surface phenology: The urban-rural gradient analysis for Chinese cities. *Glob. Change Biol.* **2021**, *27*, 2895–2904. [CrossRef]
21. Yang, J.; Luo, X.; Jin, C.; Xiao, X.; Xia, J. Spatiotemporal patterns of vegetation phenology along the urban–rural gradient in Coastal Dalian, China. *Urban. For. Urban. Green.* **2020**, *54*, 126784. [CrossRef]
22. Zhou, D.; Zhao, S.; Zhang, L.; Liu, S. Remotely sensed assessment of urbanization effects on vegetation phenology in China's 32 major cities. *Remote Sens. Environ.* **2016**, *176*, 272–281. [CrossRef]
23. Jeong, S.J.; Park, H.; Ho, C.H.; Kim, J. Impact of urbanization on spring and autumn phenology of deciduous trees in the Seoul Capital Area, South Korea. *Int. J. Biometeorol.* **2019**, *63*, 627–637. [CrossRef]
24. Lai, X.; Li, M.; Liu, C.; Zhong, Y.; Lin, L.; Wang, H. The phenological responses of plants to the heat island effect in the main urban area of Chongqing. *Acta Ecol. Sin.* **2019**, *39*, 7025–7034. [CrossRef]
25. Liu, Z.; Zhou, Y.; Feng, Z. Response of vegetation phenology to urbanization in urban agglomeration areas: A dynamic urban-rural gradient perspective. *Sci. Total Environ.* **2023**, *864*, 161109. [CrossRef]
26. Wang, L.; De Boeck, H.J.; Chen, L.; Song, C.; Chen, Z.; McNulty, S.; Zhang, Z. Urban warming increases the temperature sensitivity of spring vegetation phenology at 292 cities across China. *Sci. Total Environ.* **2022**, *834*, 155154. [CrossRef]
27. Du, H.; Wang, M.; Liu, Y.; Guo, M.; Peng, C.; Li, P. Responses of autumn vegetation phenology to climate change and urbanization at northern middle and high latitudes. *Int. J. Appl. Earth Obs. Geoinf.* **2022**, *115*, 103086. [CrossRef]
28. Jiang, Y.; Zhou, L.; Chen, Z. Climbing characteristics of typical valley-type urban construction land and its ecological quality influence. *Mt. Res.* **2022**, *40*, 570–580. [CrossRef]
29. Peng, J.; Xie, P.; Liu, Y.; Hu, X. Integrated ecological risk assessment and spatial development trade-offs in low-slope hilly land: A case study in Dali Bai Autonomous Prefecture, China. *Acta Ecol. Sin.* **2015**, *70*, 1747–1761. [CrossRef]
30. Wang, Y.; Dai, E. Spatial-temporal changes in ecosystem services and the trade-off relationship in mountain regions: A case study of Hengduan Mountain region in Southwest China. *J. Clean. Prod.* **2020**, *264*, 121573. [CrossRef]
31. Antonelli, A.; Kissling, W.D.; Flantua, S.G.A. Geological and climatic influences on mountain biodiversity. *Nat. Geosci.* **2018**, *11*, 718–725. [CrossRef]
32. Rahbek, C.; Borregaard, M.K.; Antonelli, A.; Colwell, R.K. Building mountain biodiversity: Geological and evolutionary processes. *Science* **2019**, *365*, 1114–1119. [CrossRef]
33. Misra, G.; Asam, S.; Menzel, A. Ground and satellite phenology in alpine forests are becoming more heterogeneous across higher elevations with warming. *Agric. For. Meteorol.* **2021**, *303*, 108383. [CrossRef]
34. Wang, J.; Feng, L.; Palmer, P.I.; Liu, Y.; Fang, S.; Bosch, H.; O'Dell, C.W.; Tang, X.; Yang, D.; Liu, L.; et al. Large Chinese land carbon sink estimated from atmospheric carbon dioxide data. *Nature* **2020**, *586*, 720–723. [CrossRef]
35. Yi, S. Urban mountaineering and farmers entering cities: Yunnan's path choice for protecting cultivated land. *Creation* **2011**, *9*, 30–35.
36. Ming, Q.; Wang, J.; Zhang, W. A geographical interpretation of mountain exploitation and construction of mountainous towns: A case study of Yunnan. *J. Yunnan Norm. Univ. (Humanit. Soc. Sci. Ed.)* **2012**, *44*, 48–53.
37. Yunnan Statistical Bureau. *Yunnan Statistical Yearbook 2021*; Yunnan Statistical Bureau: Yunnan, China, 2021.
38. Zhou, C.; Cheng, W.; Qian, J.; Li, B.; Zhang, B. Research on the Classification System of Digital Land Geomorphology of 1:1000,000 in China. *J. Geo-Inf. Sci.* **2009**, *11*, 707–724.
39. Huete, A.; Didan, K.; Miura, T.; Rodriguez, E.P.; Gao, X.; Ferreira, L.G. Overview of the radiometric and biophysical performance of the MODIS vegetation indices. *Remote Sens. Environ.* **2002**, *83*, 195–213. [CrossRef]
40. Ding, H.; Bu, Y.; Xu, L. Spatial and temporal variation of the plant phenology and its response to the urbanization trend in the Yangtze River delta. *J. Saf. Environ.* **2021**, *21*, 1352–1360. [CrossRef]
41. Gong, P.; Li, X.; Wang, J.; Bai, Y.; Chen, B.; Hu, T.; Liu, X.; Xu, B.; Yang, J.; Zhang, W.; et al. Annual maps of global artificial impervious area (GAIA) between 1985 and 2018. *Remote Sens. Environ.* **2020**, *236*, 111510. [CrossRef]
42. Liu, Z.; Ding, Y.; Jiao, Y.; Wang, J.; Liu, C.; Xu, Q. Spatiotemporal Variation of Impervious Surface and Abnormal Climate Phenomenon in Central Yunnan Urban Agglomeration. *Acta Geogr. Sin.* **2022**, *77*, 1775–1793. [CrossRef]
43. Cai, Z.; Jönsson, P.; Jin, H.; Eklundh, L. Performance of smoothing methods for reconstructing NDVI time-series and estimating vegetation phenology from MODIS data. *Remote Sens.* **2017**, *9*, 1271. [CrossRef]

44. Zhang, Y.; Wang, J.; Nong, L.; Cheng, F.; Zhang, Y. Spatio-temporal variation of vegetation phenology and its response to climate in the tropic of cancer (Yunnan section) based on MODIS time-series data. *Ecol. Environ. Sci.* **2021**, *30*, 274–287. [CrossRef]
45. Theil, H. A rank-invariant method of linear and polynomial regression analysis. *Indag. Math.* **1950**, *12*, 173.
46. Sen, P.K. Estimates of the Regression Coefficient Based on Kendall's Tau. *J. Am. Stat. Assoc.* **1968**, *63*, 1379–1389. [CrossRef]
47. Yue, S.; Pilon, P.; Cavadias, G. Power of the Mann–Kendall and Spearman's rho tests for detecting monotonic trends in hydrological series. *J. Hydrol.* **2002**, *259*, 254–271. [CrossRef]
48. Li, X.; Gong, P.; Zhou, Y.; Wang, J.; Bai, Y.; Chen, B.; Hu, T.; Xiao, Y.; Xu, B.; Yang, J.; et al. Mapping global urban boundaries from the global artificial impervious area (GAIA) data. *Environ. Res. Lett.* **2020**, *15*, 094044. [CrossRef]
49. Ge, M.; Feng, Z. Polulation distribution of China based on GIS: Classification of population density and curve of population gravity centers. *Acta Geogr. Sin.* **2009**, *64*, 202–210.
50. Yang, Y.; Luo, X.; Li, R.; Wang, Y.; Wen, R.; Yang, G.; Jiao, M.; Zhang, Q.; Zhang, X. A review of the effect of meteorological factors on plant phenology and its driving mechanisms. *J. Meteorol. Environ.* **2016**, *32*, 154–159.
51. Li, T.; Guo, Z.; Ma, C. Spatiotemporal changes of piedmont phenology in the transitional zone between the second and third steps, China. *Geogr. Res.* **2022**, *41*, 3000–3020. [CrossRef]
52. Oke, T.R. The energetic basis of the urban heat island. *Q. J. R. Meteorol. Soc.* **1982**, *108*, 1–24. [CrossRef]
53. Zhao, D.; Li, F.; Wang, R. Effects of ground surface hardening on plant eco-physiological processes in urban landscapes. *Acta Ecol. Sin.* **2010**, *30*, 3923–3932.
54. Xu, H.; Li, C.; Wang, H.; Zhou, R.; Liu, M.; Hu, Y. Long-Term Spatiotemporal Patterns and Evolution of Regional Heat Islands in the Beijing–Tianjin–Hebei Urban Agglomeration. *Remote Sens.* **2022**, *14*, 2478. [CrossRef]
55. Yang, Q.; Huang, X.; Yang, J.; Liu, Y. The relationship between land surface temperature and artificial impervious surface fraction in 682 global cities: Spatiotemporal variations and drivers. *Environ. Res. Lett.* **2021**, *16*, 024032. [CrossRef]
56. Flynn, D.F.B.; Wolkovich, E.M. Temperature and photoperiod drive spring phenology across all species in a temperate forest community. *New Phytol.* **2018**, *219*, 1353–1362. [CrossRef]
57. Zheng, Q.; Teo, H.C.; Koh, L.P. Artificial Light at Night Advances Spring Phenology in the United States. *Remote Sens.* **2021**, *13*, 399. [CrossRef]
58. Lindberg, F.; Grimmond, C.S.B. Nature of vegetation and building morphology characteristics across a city: Influence on shadow patterns and mean radiant temperatures in London. *Urban. Ecosyst.* **2011**, *14*, 617–634. [CrossRef]
59. Moriwaki, R.; Watanabe, K.; Morimoto, K. Urban dry island phenomenon and its impact on cloud base level. *J. JSCE* **2013**, *1*, 521–529. [CrossRef]
60. Chithra, S.V.; Nair, M.V.H.; Amarnath, A.; Anjana, N.S. Impacts of Impervious Surfaces on the Environment. *Int. J. Eng. Sci. Invent.* **2015**, *4*, 27–31.
61. Wohlfahrt, G.; Tomelleri, E.; Hammerle, A. The urban imprint on plant phenology. *Nat. Ecol. Evol.* **2019**, *3*, 1668–1674. [CrossRef]
62. Liu, Q.; Fu, Y.H.; Zhu, Z.; Liu, Y.; Liu, Z.; Huang, M.; Janssens, I.A.; Piao, S. Delayed autumn phenology in the Northern Hemisphere is related to change in both climate and spring phenology. *Glob. Change Biol.* **2016**, *22*, 3702–3711. [CrossRef] [PubMed]
63. Wang, X.; Du, P.; Chen, D.; Lin, C.; Zheng, H.; Guo, S. Characterizing urbanization-induced land surface phenology change from time-series remotely sensed images at fine spatio-temporal scale: A case study in Nanjing, China (2001–2018). *J. Clean. Prod.* **2020**, *274*, 122487. [CrossRef]